A time-resolved 128×128 SPAD camera for laser Raman spectroscopy

Yuki Maruyama[1], Jordana Blacksberg[2], and Edoardo Charbon[1]

[1]Circuits and Systems, Delft University of Technology, Delft, the Netherlands

[2]Jet Propulsion Laboratory, California Institute of Technology, Pasadena, CA, 91109, USA

ABSTRACT

In this paper we present a time-gated single-photon avalanche diode (SPAD) array, the first of its kind to be integrated with a newly developed time-resolved laser Raman spectrometer. Time-resolved Raman spectra from various highly fluorescent minerals were successfully observed using our SPAD array; these spectra were obscured by an overwhelming fluorescence background when measured using a traditional continuous wave green laser. The system has photon detection efficiency (PDE) of 5 % at 5 V excess bias with on-chip microlenses. The dark count rate (DCR) of this SPAD is 1.8 kHz at 5 V excess bias. However, thanks to the nanosecond scale time-gating, noise rate per frame is effectively reduced to ~10^{-3} counts at 40 kHz laser repetition rate.

Keywords: Time-resolved laser Raman spectroscopy, CMOS image sensor, Single-photon avalanche diode, SPAD

1. INTRODUCTION

Raman spectroscopy is a nondestructive optical analysis technique that obtains structural and compositional information from organic and inorganic samples. Thanks to its high identification performance, an *in situ* Raman spectrometer is proposed for many future planetary surface missions, for example ExoMars and Max-C rovers [1]. However, in continuous-wave (CW) laser Raman spectroscopy, significant background fluorescence often overwhelms the Raman signature. To overcome this issue, fast time-resolved laser Raman spectroscopy has been developed using a streak camera [2]. A time-resolved laser Raman spectrometer offers significant background reduction based on the temporal difference between Raman signature (virtually instantaneous) and large background fluorescence (ns ~ ms). However, such instruments require highly sensitive, high speed detectors such as intensified charge-coupled devices (iCCDs) or streak cameras. Thus, time-resolved laser Raman spectroscopy has not been used commercially, in part due to cost, size, and complexity.

Recently, a novel solution based on single-photon avalanche diodes (SPADs) has emerged as the technology of choice to create compact, time-resolved image sensors in standard complementary metal-oxide semiconductor (CMOS) process [3]. Nowadays, SPADs are available in standard nanometer scale CMOS technology [4],[5], which allows integration of high-performance circuitry and parallel data processing [6].

This paper presents an all-digital, time-gated 128×128 CMOS SPAD imager for time-resolved laser Raman spectroscopy. Raman signatures observed in this study are comparable to those obtained with existing high-end technology based on a streak camera, which requires high operating voltages, typically in the kV range. The time-gated SPAD imager offers background fluorescence rejection with a significant reduction in size and power. This simplification of the time-resolved Raman spectrometer is a great advantage for *in situ* planetary exploration.

2. A TIME-GATED SPAD CAMERA

2.1 SPAD camera system

Figure 1 shows a block diagram of the proposed sensor and a simplified optical setup for time-resolved Raman spectroscopy. A small fraction of the pulsed laser light is used as an optical trigger which is detected by a single SPAD. Timing of the trigger signal is controlled by the external delay line to activate SPADs when the Raman spectrum is projected on the image plane. A microphotograph of the SPAD imager and readout system are shown in Figure 2. The chip was fabricated in 0.35 μm high-voltage standard CMOS technology. The pixel pitch is 25 μm and the total area 20.5 mm^2. The close-up of the SPAD is shown as the figure inset. The time-gated, 128×128 CMOS SPAD imager was

first realized for on-chip fluorescence detection and fluorescence lifetime imaging microscopy (FLIM) in a time-gated mode of operation [7]. The system was modified for time-resolved laser Raman spectroscopy.
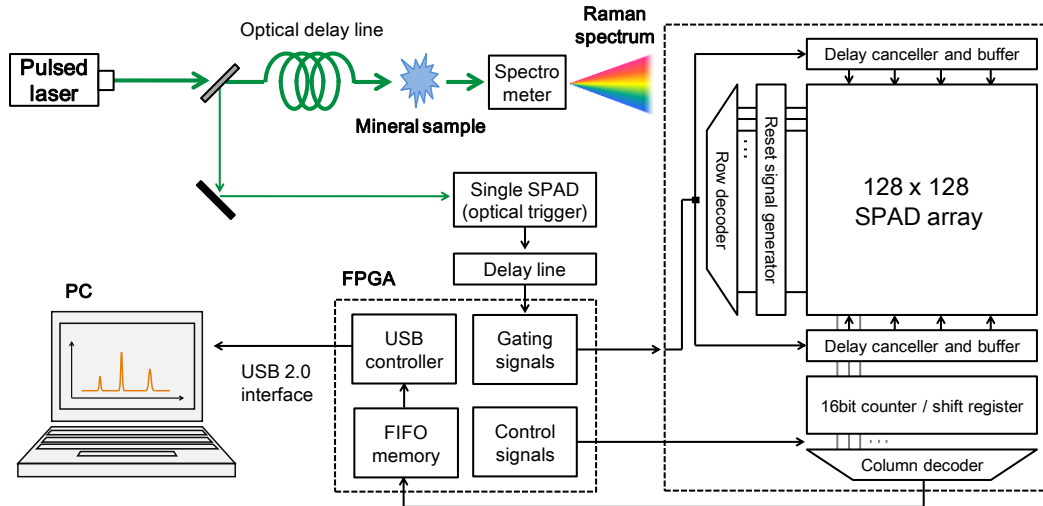

Figure 1: Block diagram of the proposed sensor and a simplified optical setup. Raman spectrum is projected on the SPAD imager. A single SPAD is used to trigger the entire camera system. Each pixel's state is stored in a 1-bit counter that is read out in rolling shutter mode, accumulated and serialized on-chip, and send to the operation computer via a FIFO memory and a USB communication module.
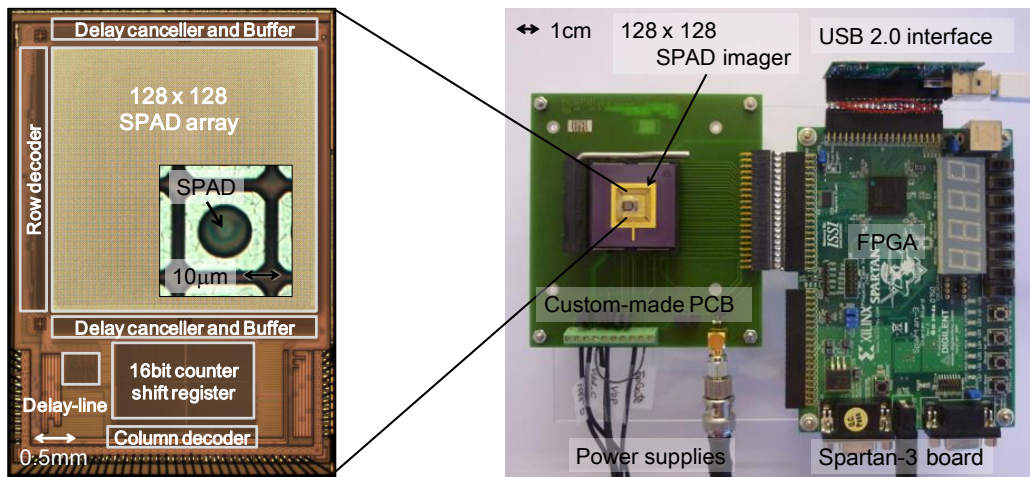

Figure 2: A time-gated SPAD camera system. (a) Photograph of the sensor chip and a readout system. The chip, fabricated in a 0.35 μm high-voltage standard CMOS process, has a total image plane area of 3.2 mm ✕ 3.2 mm. The pixel pitch is 25 μm. The inset shows close-up of the pixel without microlens.

2.2 Pixel architecture

Figure 3(a) shows a schematic diagram of the pixel. When the photon arrives at the image plane, the SPAD array is only activated by properly controlled $T_{recharge}$ followed by T_{gate}. The system has photon detection efficiency (PDE) of 5 % at 5 V excess bias with on-chip microlenses (CF=1.59). The median dark count rate (DCR) of this SPAD imager is 1.8 kHz at 5 V excess bias [8]. However, thanks to the nanosecond scale time-gating, noise rate per frame was reduced

down to ~10^{-3} counts at 40 kHz laser repetition rate. A simplified timing diagram is shown in Figure 3(b). The trigger signal enables $T_{recharge}$ to activate the entire SPAD array. Then, signal T_{gate} allows the 1-bit counter to capture the avalanche events caused by the Raman spectrum. The counter output is read out in rolling shutter mode every 409 µs. Therefore, 16 excitation laser pulses reach the sample to cause Raman spectrum emission per frame at 40 kHz laser repetition rate. Due to the low efficiency of the process, on average much fewer than 1 event per frame occur, thus several tens or perhaps hundred frames are necessary to achieve accurate and statistically relevant measurements.
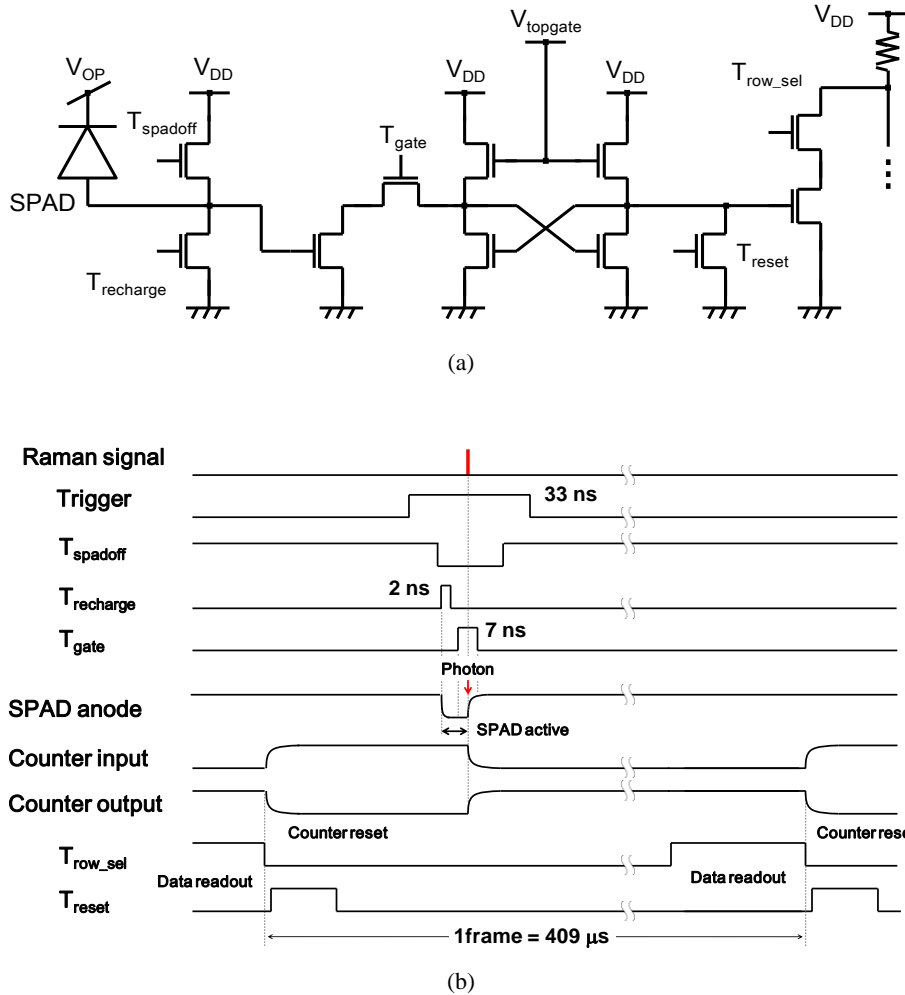

(a)

(b)

Figure 3: Schematic diagram of the pixel. (a) Overall pixel schematics including a SPAD, a 1-bit counter and a readout circuitry as well as $T_{spadoff}$, $T_{recharge}$ and T_{gate} for time-gating. (b) Simplified timing diagram of the time-gated operation for Raman spectroscopy.

2.3 Optical trigger module

Generally, passively q-switched solid state lasers have relatively large timing uncertainty. The pulsed laser used in this study has ~ 1.5 µs timing jitter. Therefore, trigger signals must be created from each laser pulse to achieve nanosecond scale gating. Figure 4(a) shows schematic diagram of the optical trigger module.
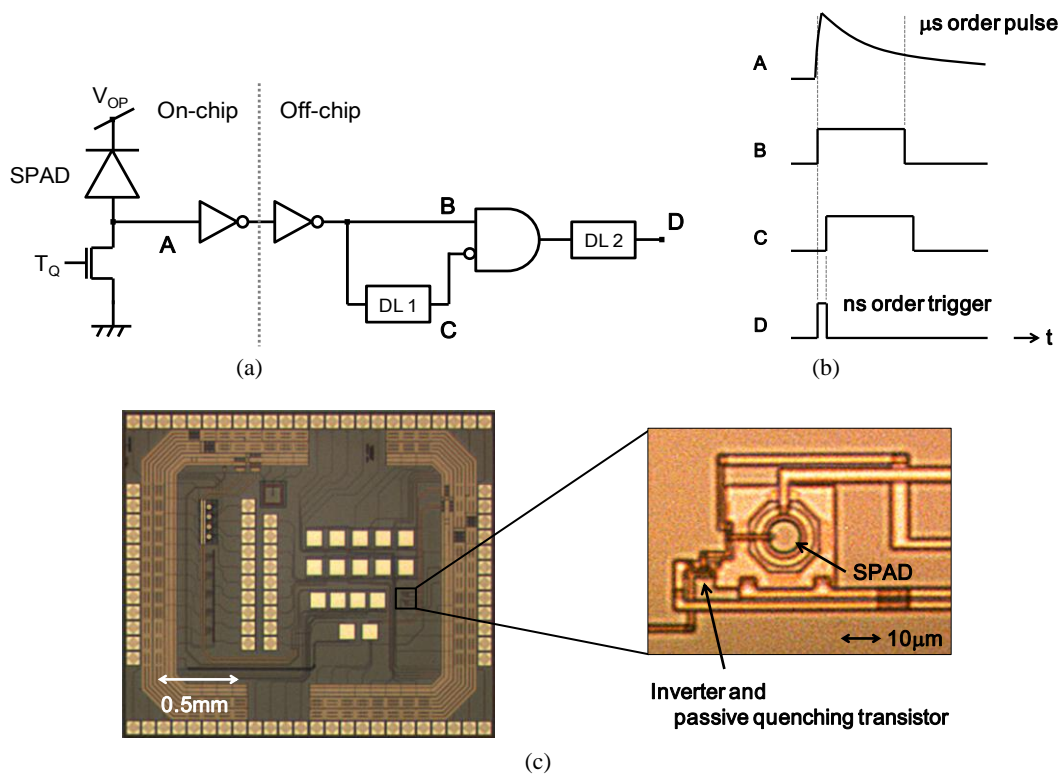
Figure 4: The optical trigger module. (a) Schematic diagram of the optical trigger module. The delay line (DL1) controls trigger width while the other delay line (DL2) controls the trigger timing. (b) Timing diagram of the trigger pulse generation. Rising edge of the μs order pulse is trimmed down to the ns order trigger pulse. (c) Photograph of the optical trigger chip and close-up of the single SPAD element. The chip was fabricated in 0.35 μm high-voltage standard CMOS technology as well as the 128×128 CMOS SPAD array.

A passively quenched SPAD output is buffered by two-stage inverters. Off-chip delay lines control the trigger width and its timing to activate the SPAD camera when the Raman spectrum is arriving at the image plane. The rising edge of the inverter output was trimmed by a NAND gate as shown in Figure 4(b). A SPAD dead time was set at 1 ms to minimize afterpulses, which have negligible probability at the levels used during dead time. Figure 4(c) shows a microphotograph of the trigger chip and close-up of the passively quenched SPAD as well as an integrated inverter.

3. DETECTOR PERFORMANCE

3.1 Noise and sensitivity

The sensor was first characterized in terms of its noise and sensitivity. To operate SPADs in Geiger mode, a reverse bias voltage was applied to the SPADs in excess of its breakdown voltage of 19.1 V. Figure 5(a) shows the dark count rate (DCR) cumulative probability plotted for different excess bias voltages (Ve) from 2.5 V to 4 V at room temperature. The median DCR of this chip, 53 Hz with Ve=3 V, is superior to that measured in [9]. The proportion of noisy pixels (DCR > 1 kHz) is 1.53 % with Ve=4 V, is significantly lower than that of [10]. We assume that the in-pixel 1-bit counter plays a role in filtering afterpulses, since the memory stores only the first avalanche event in each frame. This feature offers significant improvement in the image quality when the incident photon number is extremely low. Figure 5(b) plots the photon detection probability (PDP), as well as the photon detection efficiency (PDE) at different excess biases. A peak PDP of 43.6 % at 475 nm was observed with Ve=4 V.
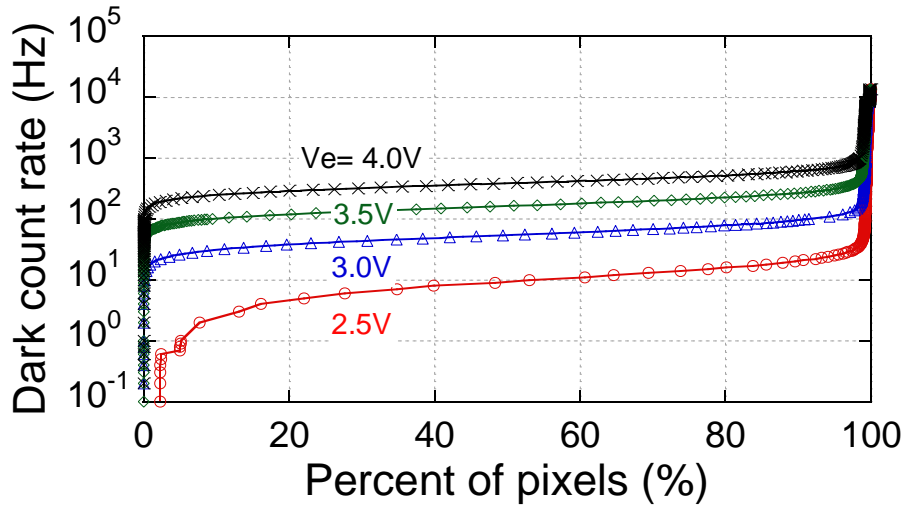
(a)
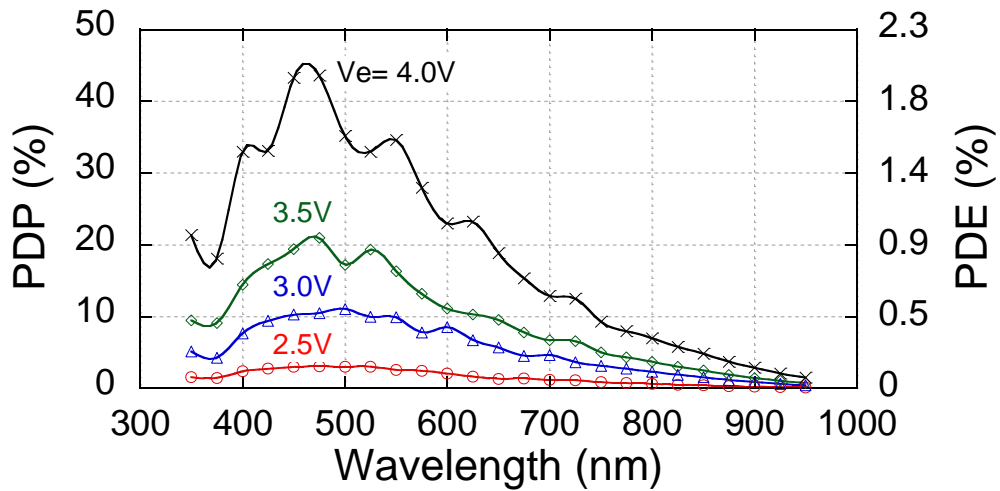
(b)

Figure 5: Basic characteristics of the time-gated SPAD camera. (a) Cumulative dark count rate (DCR) for the pixel population of the entire array (16,384 pixels). (b) Median photon detection probability (PDP) and photon detection efficiency (PDE) of the entire array at different excess bias conditions without microlenses. PDE was calculated as PDP × fill factor (4.5 %). All measurements were performed at room temperature.

3.2 On-chip microlens

For further improvement of PDE, on-chip microlenses were fabricated directly on the sensor surface. Figure 6(a) shows the concentration factor (CF) map across the entire chip. Due to a misalignment that occurred during fabrication of the microlenses, CF varies from 1 to 3 as shown in Figure 6(b). The measured median concentration factor is 1.59 which improves the PDE of the SPAD camera. This issue will be solved by increasing the sensor size and optimizing the microlens fabrication process. We believe that the microlens array can be improved to achieve its theoretical value of 15.
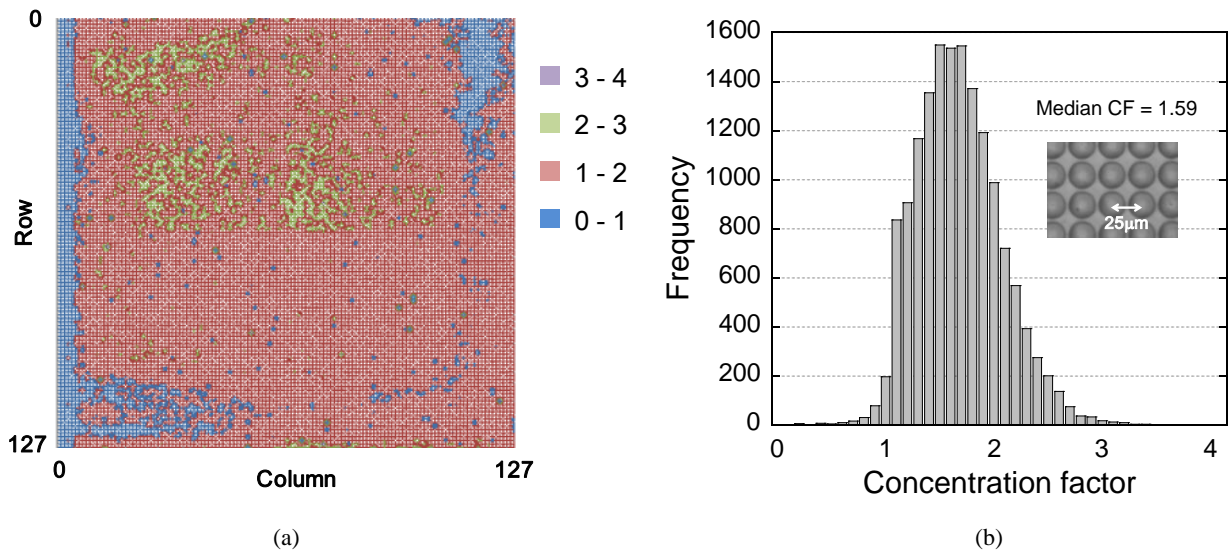
(a)

(b)

Figure 6: The concentration factor (CF) of the on-chip microlens array. (a) The CF distribution across the entire chip. (b) Histogram of the CF. The CF value varies from 1 to 3 due to the alignment and height issues. The inset shows a microphotograph of circular shaped microlenses. Square microlenses (not shown here) have also been fabricated.

4. EXPERIMENTAL RESULTS

4.1 Experimental setup

Figure 7 shows block diagram of the simplified experimental setup. The time-resolved Raman spectroscopy instrument was originally designed for detection using a streak camera [2]. Simple modifications to the setup allowed us to replace the streak camera with our SPAD imager. Table 1 summarizes experimental parameters.
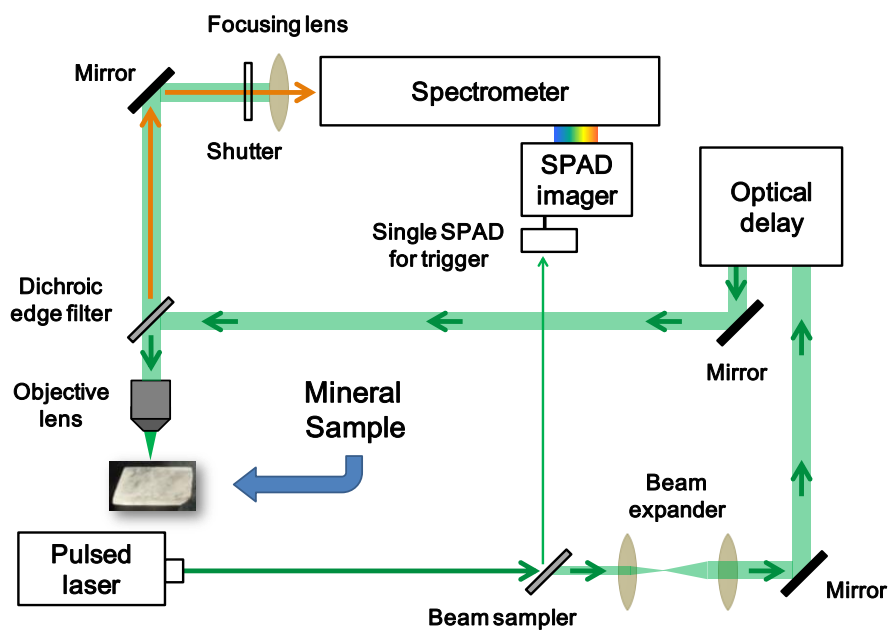

Figure 7: Block diagram of the simplified time-resolved Raman spectrometer setup.

Table 1. Experimental Parameters	
Laser Wavelength	532 nm
Laser Pulse Energy	1 μJ/pulse
Laser Pulse Width	500 ps
Laser rep rate	40 kHz
Time per frame	409 μs
Frames per measurement	10,000 (typical)
Image plane size	3.2 mm × 3.2 mm
Pixel size	25 μm × 25 μm
SPAD on time	7 ns
Trigger width	33 ns
SPAD breakdown voltage	19.1 V
SPAD excess bias	5 V
SPAD dark count rate (DCR)	1830 Hz (at 5 V excess bias)
Microlens concentration factor	1.59 (median)
Photon detection efficiency (PDE)	5 % (at 5 V excess bias)
Power consumption	360 mW (at V_{dd} = 2.5 V)

4.2 Time-resolved Raman spectra

Initial time-resolved Raman spectroscopy experiments were performed using natural calcite minerals since calcite has a clear and intense Raman return. Figure 8 shows an example of the sensor output integrated over 10,000 frames at room temperature. The Raman spectra were successfully observed with high signal-to-noise ratio (SNR) without any cooling system, which is commonly used in CCD based CW Raman spectrometer designed for *in situ* planetary exploration [11],[12].

As a demonstration of the large fluorescence rejection capabilities of this system, we measured the natural mineral willemite which has very intense green fluorescence. In this mineral, Raman spectra are completely obscured by this large fluorescence in the absence of time gating. Figure 9 shows the Raman spectra observed from willemite at different time-gating window. Significant background fluorescence was suppressed by reducing the time-gating window from > 1 μs to < 33 ns. It should be noted that the minimum gating time that was achieved using this chip (33 ns) is not an intrinsic limitation. This timing was chosen when the chip was originally designed for the FLIM application. Future work will focus on optimizing this chip for time-resolved Raman, and we expect that sub-ns gating will be possible.

In addition to Raman spectroscopy, the proposed time-resolved laser spectrometer is also applicable to fluorescence spectroscopy and Laser Induced Breakdown Spectroscopy (LIBS), providing complementary elemental information [13]. Thanks to the fluorescence background elimination effect of the time-domain filtering, a 532 nm pulsed laser can be used for combined Raman, fluorescence and LIBS. Therefore, the volume/mass can be further more reduced compared to that of combined Raman/LIBS instruments using two different lasers [12].
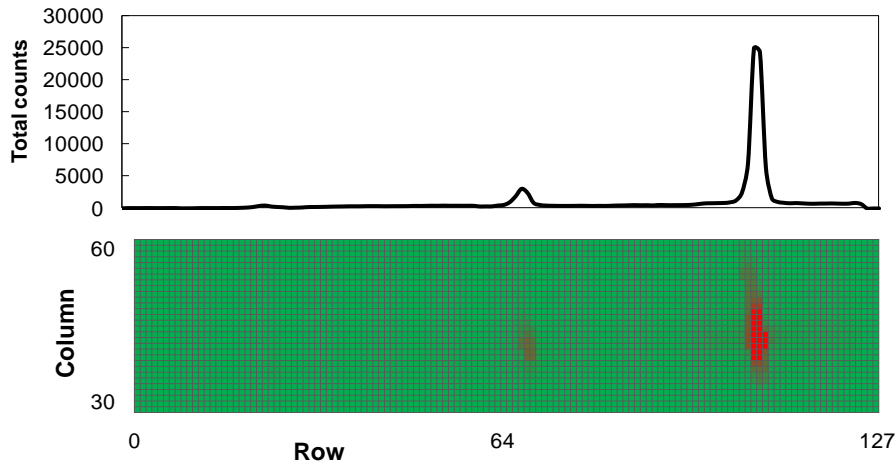
Figure 8: A time-gated SPAD camera output of natural calcite spectrum (false color). The gating time of this experiment was 33 ns. A broadband grating (resolution: ~ 10 cm^{-1}) was used to observe wide range of the Raman spectrum within 3.2 mm wide image plane. The wavenumber resolution will be improved in future work.
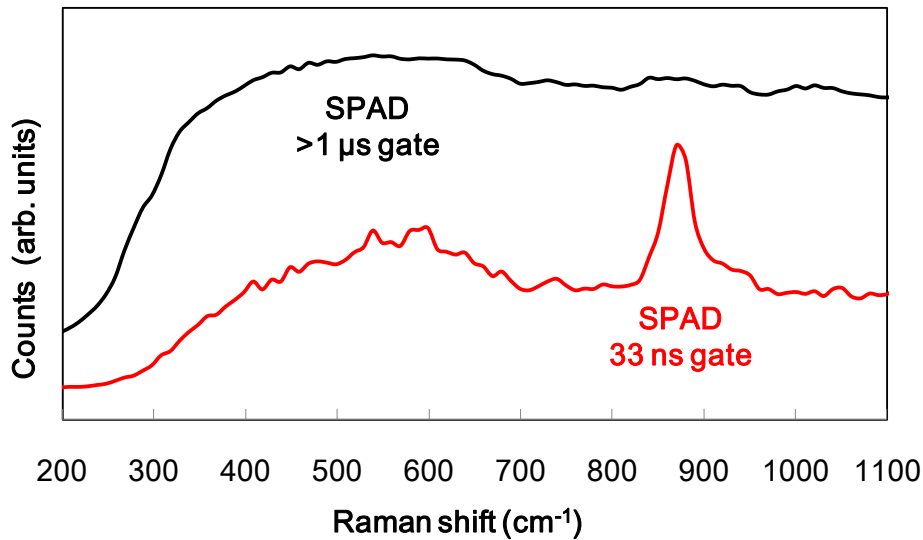

Figure 9: Raman spectra from willemite at different time-gating windows using the proposed SPAD camera. Thanks to the nanosecond scale gating, overwhelming fluorescence was successfully suppressed. Overwhelming fluorescence was not suppressed by microsecond-gates or longer. The time-resolved imaging allows us to observe Raman spectra from highly fluorescent sample which were impossible to extract the Raman signature using traditional CW Raman spectroscopy.

5. CONCLUSIONS

Time-resolved Raman spectra from highly fluorescent mineral samples were successfully observed using our SPAD array; these spectra were obscured by an overwhelming fluorescence background when measured using a traditional continuous wave green laser. The SPAD imager has various advantages compared to a traditional photocathode-based imager system, such as smaller size, lighter weight, lower operation voltage, less power dissipation, and greater radiation hardness. These valuable features will help us to develop portable, fully automated, time-resolved single-photon

detectors. The integration of the SPAD imager with a laser Raman instrument can provide enhanced capability in various fields such as mineralogy, archaeology, medical science, and planetary science, where rapid and non-destructive material identification on a microscopic scale is required.

ACKNOWLEDGEMENTS

REFERENCES

[1] Grant, J.A., Westall, F., and the MEPEG 2R-iSAG team., "Tow rovers to the same site on Mars, 2018: possibilities for cooperative science," Astrobiology 10, 663-685 (2010).

[2] Blacksberg, J., Rossman, G.R., Glecker, A., "Time-resolved Raman Spectroscopy for in situ planetary mineralogy," Appl. Opt. 49(26), 4951-4962 (2010).

[3] Rochas, A., Gani, M., Furrer, B., Basse, P.A., and Popovic, R.S., "Single Photon Detector fabricated in a Complementary Metal-oxide-semiconductor High-voltage Technology," Rev. Sci. Instrum. 74, 3263-3270 (2003).

[4] Karami, M.A., Gersbach, M., Yoon, H., and Charbon, E., "A new single-photon avalanche diode in 90nm standard CMOS technology," Opt. Express, 18 (21), 22158-22166 (2010).

[5] Richardson, J.A., Webster, E.A.G., Grant, L.A., and Henderson, R.K., "Scalable Single-Photon Avalanche Diode Structures in Nanometer CMOS Technology", IEEE Trans. Electron Dev., 58 (7), 2018-2035 (2011).

[6] Veerappan, C., Richardson, J., Walker, R., Day-Uey Li, Fishburn, M.W., Maruyama, Y., Stoppa, D., Borghetti, F., Gersbach, M., Henderson, R.K., Charbon, E., "A 160×128 single-photon image sensor with on-pixel 55ps 10b time-to-digital converter", Proc. ISSCC, 312-314 (2011).

[7] Maruyama, Y., and Charbon, E., "A time-gated 128×128 CMOS SPAD array for on-chip fluorescence detection," Proc. IISW, 270-273 (2011).

[8] Blacksberg, J., Maruyama, Y., Charbon, E., Rossman, G.R., "Fast single-photon avalanche diode arrays for laser Raman spectroscopy," Opt. Lett. 36 (18), 3672-3674 (2011).

[9] Niclass, C., "Single-Photon Image Sensors in CMOS: Picosecond Resolution for Three-Dimensional Imaging," Ecole Polytechnique Fédérale de Lausanne, Ph.D. thesis dissertation, no. 4161 (2008).

[10] Stoppa, D., Mosconi, D., Pancheri, L., and Gonzo, L., "Single-Photon Avalanche Diode CMOS Sensor for Time-Resolved Fluorescence Measurements," IEEE Sens. J. 9 (9), 1084-1090 (2009).

[11] Ingley, R. Hutchinson, I.B., Edwards, H.G.M., Moral, A.G., Diaz, E., Ramos, G., Barcos, O., Canora, C.P., Rull, F., Tato, C., Pool, P., "ExoMars Raman Laser Spectrometer Breadboard: Detector Design and Performance," Proc. SPIE 8152, 815215-815215-9 (2011).

[12] Ahlers, B., Hutchinson, I., Ingley, R., and Raman LIBS EBB team., "Combined Raman/LIBS Spectrometer Elegant Breadboard – Built and Tested – and Flight Model Spectrometer Unit," Proc. 7th Int. Conf. on Space Optics (2008).

[13] Blacksberg, J., Maruyama, Y., Choukroun, M., Charbon, E., Rossman, G.R., "New Microscopic Laser-coupled Spectroscopy Instrument Combining Raman, LIBS, and Fluorescence for Planetary Surface Mineralogy," Proc. 43rd Lunar and Planetary Science Conference, 1510 (2012).